Araştırma Makalesi
Bayburt Üniversitesi Fen Bilimleri Dergisi
Cilt 2, Sayı 1

Geliş Tarihi: 01.03.2019
Kabul Tarihi:21.05.2019

dergipark.gov.tr/bufbd

Gain Increase of Horn Antenna with Waveguide Feeding Network by using 3D Printing Technology

Abdullah GENC*

Isparta University of Applied Sciences, Department of Mechatronics Engineering, Isparta, Turkey

Keywords:

Horn antenna, T-junction Waveguide, 3D printing technology, 3D printer, Gain

Abstract

2×1 array antenna with WFN (waveguide feeding network) by using 3D printing Technology and metal plating technique at X-Ku frequency band is proposed in the areas of radars, defense industry and satellite communication to increase antenna gain. The fabrication of 2×1 array antenna comprises of two processes which are to produce the structure of array antenna by using ABS for 3D printer and to carry out copper plating. Waveguide feeding network for array consists of an H-plane T-junction, two bend elements and three flanges. The spacing between the output terminals in the waveguide feeding network is 3λ for better performance. There is a good agreement between measurement and simulation results by max 0.5dB difference because of surface roughness and high precision. The gain is increased by approximately1.5dB in comparison with a single antenna. However, VSWR of the single antenna is 0.3dB lower than the array antenna. As a result, we have proposed the array antenna 90% lighter weight and 80% cheaper than metal equivalents.

1. INTRODUCTION

Horn antennas have mostly been utilized in the areas of radars, defense industry, and satellite communication because of wide bandwidth, easy production, high efficiency, its simplicity and high directivity [1]. It may be used both as a standard measurement antenna in order to make calibrations and as a feeding element for reflector antennas in satellite systems. Radiation characteristic of a horn antenna is a combination of H-plane and E-plane sectorial horn antennas and they have linearly polarized radiation [2]. Also, array horn antennas are widely preferred for radar systems and satellite communications to increase the gain [3].

There has currently been an increasing concern about additive manufacturing (AM) to fabricate some monolithic passive microwave components with cost competitiveness and production time [4]. In various publications from literature, the methods of AM have increasingly been utilized in many applications such as Luniburg lenses [5], corrugated horn antennas [4], patch antennas [6], frequency selective surfaces (FSS) [7] and metamaterials [5]. The fabrication of microwave passive components and pyramidal horn antennas with fused deposition modelling (FDM) technique is a better solution due to monolithic structure, flexible applicability, and reduced weight. In traditional methods, passive microwave components are mostly produced from some metals by means of CNC machines and it is rather costly and difficult in order to fabricate the structures having the complex geometries [8-9]. Thanks to the development of 3D printing technology nowadays, the components fabricated by this technology can compete with equivalent products in the market commercial in terms of better performance and low price.

There are many publications in the literature to deal with the fabrication of the horn antenna and passive microwave components such as T-junction, E-type bend and twist elements by using the 3D additive manufacturing. In [10], Ka-band light-weight horn array antenna with 3D printing technology has been proposed. In the proposed linear-polarized 2x2 element array antenna, the T-junction, twist and the rectangular-circular waveguide transition elements are used for the feeding network that is monolithic, which is a great innovation in terms of cost and durability. The twist element is used to turn the polarization direction from horizontal to vertical. While the gain of the single horn antenna is 16dBi, it is observed that the gain of the entire array antenna was significantly increased to nearly 24dBi. In [11], 4x4 horn array antenna and feeding network

*e-Posta: abdullahgenc@isparta.edu.tr

in Ku band are designed. The rectangular waveguide operating in TE_{10} mode in the 13.5-14.5GHz range is designed to be small enough to suppress higher modes. A rectangular grid structure on each antenna's aperture is used to overcome unwanted beams. The radiating pattern of the array antenna is obtained by multiplying the radiating pattern of the single-element horn antenna with the array factor. The gain of the single horn antenna and the array antenna is 14.25dB and 27.5dB respectively.

In [12], a light-weight, monolithic horn array antenna is designed and manufactured in the Ka (26.5-40GHz) band. The structure produced using additive manufacturing consists of a conical horn antenna and a feeding network. Thanks to the 2x2 array antenna, the gain is increased by approximately 6dB. The array factor is an important parameter, which has been observed to be a distance of 3λ between the array elements in order to minimize this. Determination of the smaller distance is not possible due to the physical size of the feed network. As the number of array elements increases, the directivity of the main beam increases, while the production cost and the physical size increase, and this is often undesirable. In [13], the corrugated conical horn antenna is designed and manufactured in Ku band with 3D printer technology. Corrugated conical horn antennas are used as a feed on reflective antennas due to their low side lobe level and sharpness in polarization. The proposed structure is carried out in eight hours using ABS thermoplastic material with Fortus-250MC three-dimensional printer. Then the surface is coated with conductive nickel spray paint. Surface resistance ranges between 0.3-6Ω/sq. It is observed that surface resistance negatively affected the gain of the antenna. In the measurement results, the maximum gain is 19.6dB at 16GHz and the VSWR is about 1.92:1 at the 11-18GHz frequency range.

In [14], a ring-focus dual-reflector antenna and a spline profile smooth horn antennas are produced with three-dimensional printers with a robust dielectric material. Then, a copper coating is performed on the surface. Stereolithography is the technique underlying the 3D printers used for rapid prototyping. By this way, there is a significant improvement in weight and cost. Simulation of the proposed design, GRASP10 full wave simulator production and measurements are made in SWISSto12 laboratories in Switzerland. It has a 25dB gain at 14.5GHz. The loss of recycling is unfortunately not fully compatible between the simulation and the measurement results because there are losses due to the transducer between rectangular and circular waveguides in the feeding.

In this study, 2×1 horn array antenna having waveguide feeding network (WFN) fabricated from metal plating and 3D printing is proposed. Waveguide feeding network for array consists of an H-plane T-junction, two E-type bend and three flanges. The antenna is fabricated after each component of WFN is designed and optimized. The overall structures are produced by using fused deposition modelling (FDM) technique that is one of the additive manufacturing methods. The parameters of antenna such as directivity, radiation pattern and VSWR for both array antenna and single horn antenna are obtained. There is a fine agreement between the results of measurement and simulation. Unlike the studies in the literature, iris and septum for the impedance matching are used to design T-junction components. Also, the feeding network of the 2x1 array antenna has a novelty in this study.

This study can be organized as below. Second Section explains how to design the single horn antenna. The third Section also gives the design of WFN comprising the designs of bend element and T-junction. The fourth Section mentions the fabrication of the array antenna by using metal plating and 3D printing. The fifth Section explains the measurement and simulation results for both the array antenna and the single antenna. Sixth Section contains the conclusion and summary of the obtained results.

2. THE DESIGN OF SINGLE HORN ANTENNA

The other method is utilized curve fitting technique which has more accurate results than others. Therefore the technique of curve fitting is preferred in this paper. Other calculation method is based on optimization technique [15, 16]. Iteration technique is used at the method [1]. In this paper, the calculation of dimensions of pyramidal horn antennas is made for 12GHz operating frequency at 10-15GHz frequency range that is favourable for satellite communications. WR-75 rectangular waveguide for the overall design is preferred and the internal size of it is 19.05mm and 9.52mm. Cut-off frequency (f_c) for TE_{10} mode is specified as 7.886GHz and the size of the waveguide are calculated by using Equation 1 as a = 19.05mm and b = 9.52mm. The operating frequency varies between $1.25\ f_c < f < 1.89\ f_c$.

$$(f_c)_{mn} = \frac{1}{2\sqrt{\mu\varepsilon}}\sqrt{\left(\frac{m}{a}\right)^2 + \left(\frac{n}{b}\right)^2} \quad (1)$$

where *n* and *m* are the order number of the electromagnetic wave modes and *a* and *b* are size of the waveguide. The shape of single antenna is depicted in Figure 1.

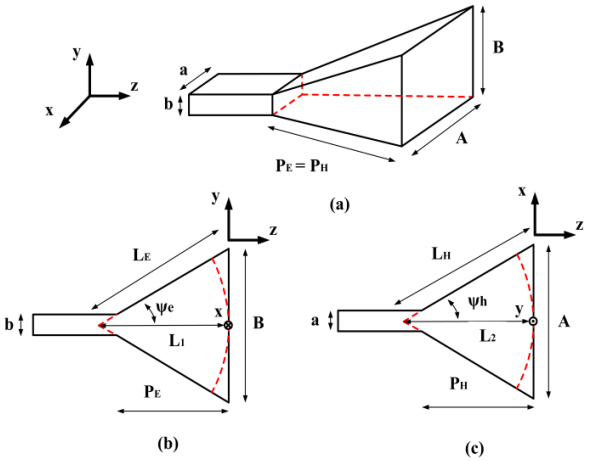

Figure 1. Single antenna (a) perspective view, (b) y-z plane, (c) x-z plane

According to Figure 1, P_E or P_H is the spacing between antenna's aperture and waveguide and *A*, *B* are aperture distance of horn antenna. The size of the horn antenna is calculated from the gain of the antenna, the internal dimensions of waveguide and resonance frequency to ensure 17dB gain at 12GHz. All dimensions are specified with an interface of Matlab GUI by using the technique of curve fitting. The spacing between the waveguide and the aperture and the aperture size of the horn are 70mm and 70.91mm×49.07mm, respectively.

3. THE DESIGN OF WFN

There are several ways to feed the array antennas. The limiting factors for the design are bandwidth and efficiency. For high efficiency, it is necessary to make a low lossy feed network. A rectangular waveguide due to a low loss is preferred in order to design WFN. The proposed WFN having three ports consists of three flanges, a T-junction and two bend elements. The array antenna is fabricated after each component of WFN is designed and optimized. The view of the waveguide feeding network with sub-component is given in Figure 2.

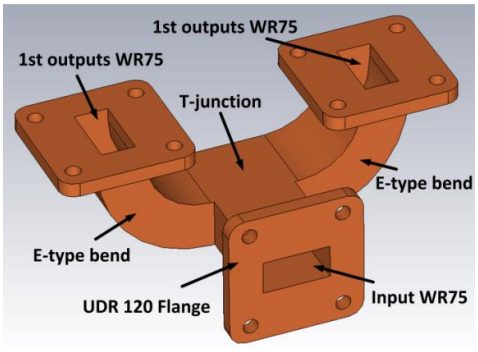

Figure 2. The view of WFN

3.1. Design of the T-Junction and Bend Components

The geometry of T-junction containing equal phase and amplitude between outputs terminals are designed in the paper [17]. The view of T-junction is depicted in Figure 3. All parameters for the design are optimized by using parametric sweep in CST program in order to have a good performance. We aim to design T-junction with equal and in-phase power division. Therefore, septum and two irises are symmetrically placed inside the T-junction. The power of EM waves at the output terminals is equal. Also, it has no phase difference between the output terminals. Finally, the size of septum and iris are obtained as (in all mm): D = 9.43, W = 2, t = 1.42, R = 1.42 d_{offset} = 9.52 and l_t = 40.

E-type bend is preferred in waveguide feeding network because it is better than sharp E-type corner in terms of performance [18]. In order to make sure that the spacing of each antenna is 3λ for 12GHz, the radius of bend element is tuned.

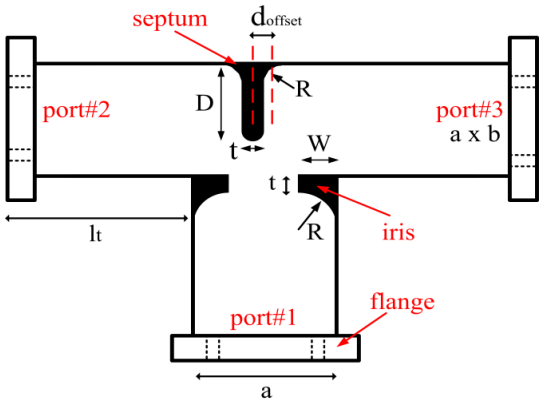

Figure 3. The view of T-junction

3.2. Array Factor of Planer Arrays

AF of planer structure is calculated by using the array number (N_x, N_y) and the distances (dx, dy) between elements. The feeding of each antenna is made in equal phase and amplitude. The array factor can be shown as a function in terms of azimuth angle φ, evaluation angle θ and N, number of array. The array factor for equal spacing is given in Equation 2.

$$|AF| = \left|\frac{\sin(N_x(\frac{2\pi}{\lambda} dx\ \sin\theta\cos\varphi))}{\sin(\frac{2\pi}{\lambda} dx\ \sin\theta\cos\varphi)}\right| \left|\frac{\sin(N_y(\frac{2\pi}{\lambda} dy\ \sin\theta\sin\varphi))}{\sin(\frac{2\pi}{\lambda} dy\ \sin\theta\sin\varphi)}\right| \quad (2)$$

In this paper, $dx = 3\lambda$, $N_x = 2$ and $N_y = 1$ is specified for the proposed 2×1 array antenna. From Equation 2, the amplitude of AF for different numbers of arrays is obtained and depicted in Figure 4. The gains of the 4×2, 2×2 and 2×1 array are bigger than that of single one by 8.38dB, 6.02dB, and 3dB. It is significant to note that the gain is independent of what kind of antenna is used and it is quite difficult to have these gain values in measurements because of the losses. As the antenna's number elements increases, beamwidth at the radiation pattern become narrower and the directionality increases. Although it is expected that the gain of 2×1 arrays theoretically increase is 3dB, the increase of the measured gain for 2×1 arrays is equal to 1.5dB in Figure 4.

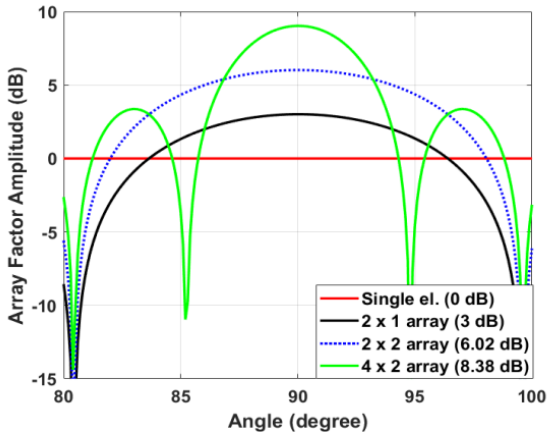

Figure 4. Amplitude of AF for different arrays

The spacing between the output terminals in the waveguide feeding network is 3λ for lower grating lobe. Element spacing in an array antenna could be multiples of 1.5λ [19]. For the spacing wider than 3λ, it is known that grating lobe rather increases. For the spacing smaller than 3λ, it is very hard to assemble T-junction component and E-type bend component in the waveguide feeding network.

In order to have a better performance of the antenna, the distance between the output terminals is 3λ in the waveguide feeding network. Element spacing in the array antenna can be multiples by 1.5λ [19]. If the distance becomes wider than 3λ, the level of grating lobe rather increases. However, if the distance becomes narrower than 3λ, it is not possible to fix the E-type bend and T-junction in the waveguide feeding network.

4. THE FABRICATION OF HORN ARRAY AND WFN

The fabrication of 2x1 array antenna comprises of two processes which are to produce the structure of array antenna by using thermoplastic and to make metal plating on the structure's all surface. Whole elements having complex geometry could be easily fabricated thanks to this method. The significant parameters for good performance are low surface roughness and high precision, especially at X-Ku frequency band. The negative impact of the surface roughness on the performance can be reduced since the wavelength is further decreased in low-frequency bands such as S and C band.

4.1. 3D Printing from Acrylonitrile Butadiene Styrene (ABS)

After we calculate all dimensions of the array antenna, the CAD model of it is obtained via CST simulation program. STL file of CAD-model is obtained from CST and the G-code file is created by using the Repetier-Host program to be compatible with the 3D printer. Zortrax M200 model 3D printer is utilized and white Acrylonitrile Butadiene Styrene is used as material for the 3D printer and the melting temperature of the plastic is 245°C and also the fill rate is 80%. The thickness of the waveguide wall is specified as 2mm to make physically it more robust. In addition, many parameters such as creating the support for cavities, layer height, first layers' number, shell thickness, working speed and type of pattern must be set before the printing.

4.2. The Process of Copper Plating

Thermoplastic such as Acrylonitrile Butadiene Styrene is not electrically conductive. Thus, the electroless plating and electro-plating technique are utilized to make the surface of the components conductive. There is a limitation of electroless plating. This technique has the advantage so that it has freedom in copper plating in the complicated geometries [20]. The copper plating consists of some stages which are etching, Pd-Sn activation, electroless nickel, acceleration, and acidic copper plating, respectively. The conductivity of copper is higher than that of nickel and chromium. So, the performance of the copper-coated antenna used is better. The thickness for the electroless one is approximately equal to 3-4μm. Then the surfaces of that are conductive. Finally, the electroplating is made on the copper layer till 20μm ±10%.

5. RESULTS AND DISCUSSION

The simulations results are obtained via CST program by using FIT Technique. In all simulation, the shape of the mesh is hexahedral, mesh per wavelength is 20. Mesh cells numbers of single antenna and 2×1 horn array antenna are 3,307,100 and 13,636,720, respectively. Lossy copper as a metal is preferred and open space as a boundary condition is used and the type of feeding is the waveguide port. The CST simulations were performed on a PC having an Intel Core i5 2.4GHz processor and 8GB RAM. The calculation times for each one take roughly 8min and 52min.

The measurement setup for the array antenna is given in Figure 5. Also, the same measurement environment is used during the study in the literature [21]. PE9819 model waveguide adaptor and an E8363B Agilent model vector network analyzer (VNA) are utilized to measure the antenna performance in the anechoic chamber. An SH2000-072 double-ridged horn antenna is preferred as a reference antenna and the distance between T_x and R_x is roughly 110cm.

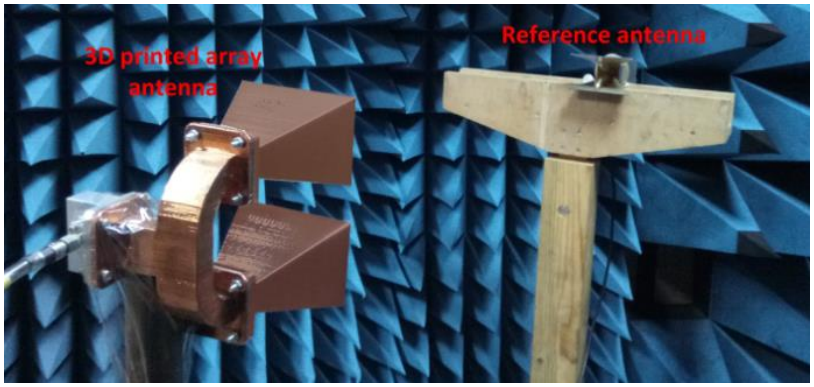

Figure 5. Measurement setup

5.1. Results for Single Antenna

The photos of single antenna for each process are depicted in Figure 6.

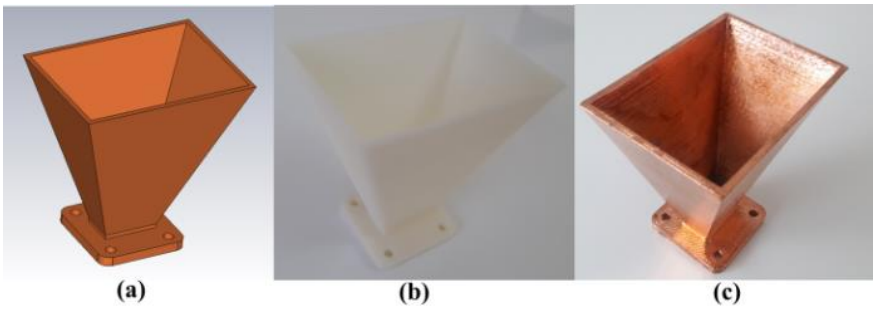

Figure 6. Single antenna (a) CST view, (b) 3D printing, (c) copper plating

The gain and VSWR of the single antenna with copper plating is depicted in Figure 7. VSWR of that is rather good, which is equal to approximately 1.35. It seems a small difference between the simulation and the measurement because of physical tolerance of the antenna and the surface roughness [22, 23]. As the frequency becomes higher, the gain of the antenna becomes higher. The gain of the single antenna varies from 16-18dB and there is a 0.5dB difference between simulation and measurement. E-plane ($\emptyset$ = 90º) radiation pattern of the antenna in polar coordinates is given in Figure 8. The antenna gain is 17.1dB at 12GHz and the direction of the main lobe is adjusted towards +z axis. The 3dB beamwidth is 25.7º and the side lobe value is around -13.3dB and it seems that the side lobe value of antenna for H-plane is less than that for E-plane.

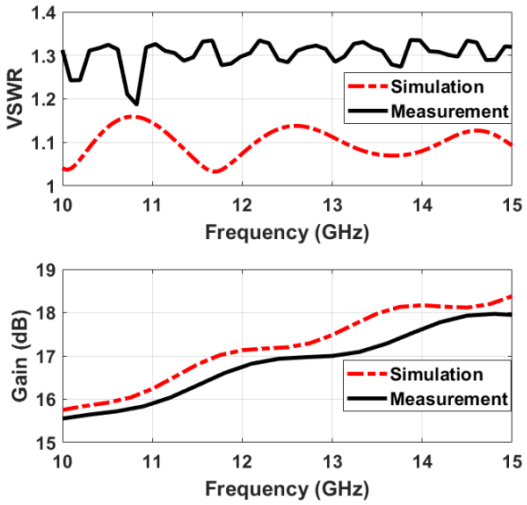

Figure 7. VSWR and gain of single horn

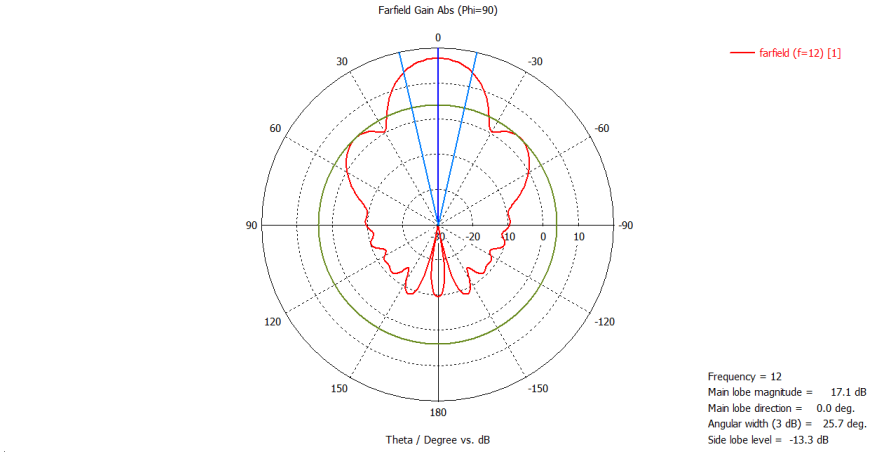

Figure 8. E-plane pattern for single antenna in polar coordinates

The normalized gain of the single antenna at 12GHz is depicted in Figure 9a. Cross polarization level in the normalized gain is lower than -40dB for all frequency range. We have a good agreement between measurement and simulation results in terms of co-polarization. Here, the directions of co-polarization and the cross polarization are in the +y and +x directions. The aim of the design is to increase co-polarization while decreasing the cross-polarization level.

H-plane (Ø = 0°) radiation patterns of single horn at 11GHz, 12GHz and 13GHz is depicted in Figure 9b. Here, as the frequency increase, both the gain increases and the beamwidth decrease.

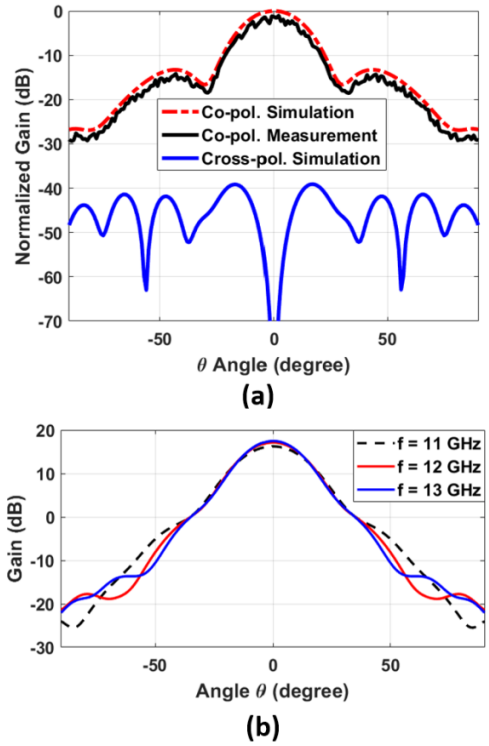

Figure 9. (a) Normalized gain for the single antenna @12GHz (b) H-plane radiation patterns of single horn

5.2. Results for 2x1 Array Antenna

The photos of 2×1 array antenna for three processes are depicted in Figure 10. This array antenna consists of two identical horn antennas and waveguide feeding network. The distance between the two antennas is roughly 3λ. We aim to maximize the single antenna's gain by using array antenna compared to single element horn antenna.

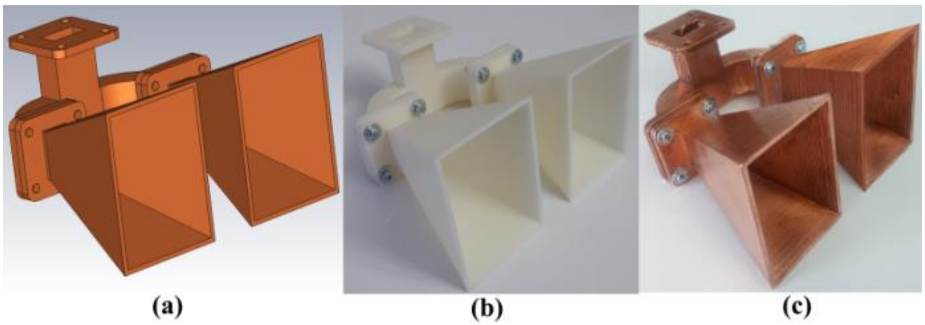

Figure 10. 2x1 array antenna (a) CST CAD model, (b) 3D printing, (c) Copper plating

The gain and VSWR of the horn antenna array is depicted in Figure 11a. The gain increases as increased frequency and it varies between 17 and 19.5dB. The VSWR is roughly 1.65. However, VSWR of the 2x1 array is increased by roughly 0.3dB. The simulated gain is 1dB bigger than the measured gain. The simulated gain value for 12GHz is 18.5dB. The simulated gain of array antenna is 1.5dB bigger than that of single antenna.

The normalized gain of the array antenna at 12GHz is given in Figure 11b. The cross polarization of antenna is lower than -30dB in all frequency band. The gain for the 2x1 array increased from 17dB to 18.8dB at 12GHz.

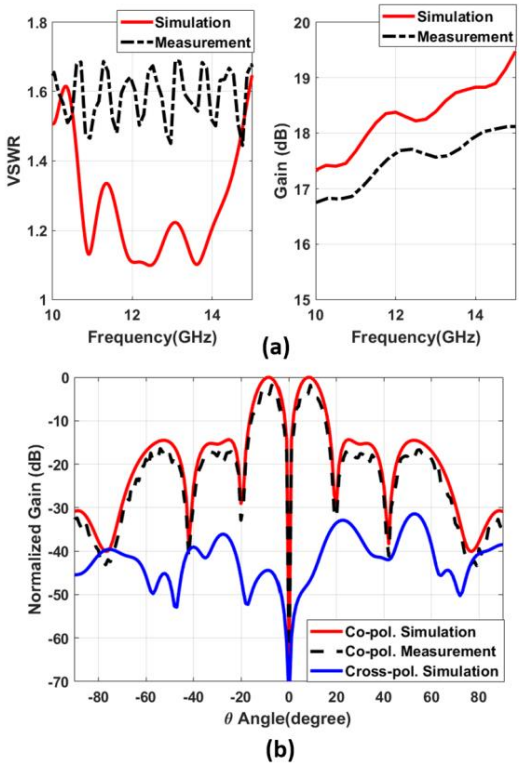

Figure 11. (a) VSWR and gain of 2x1 array (b) Normalized gain the array antenna @12GHz

3D E-field patterns of 2×1 array antennas and single antenna are given in Figure 12. A single antenna has more uniform 3D radiation pattern.

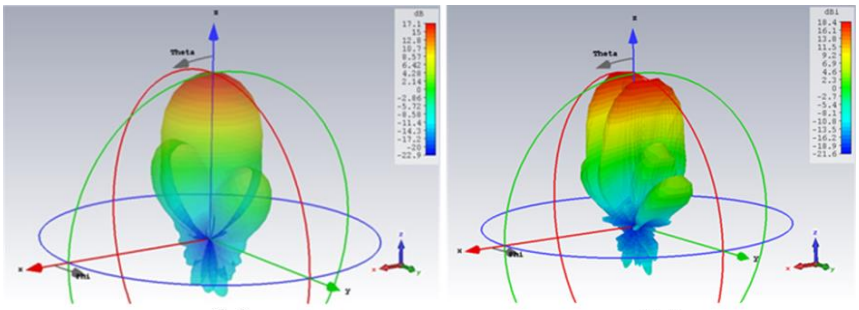

Figure 12. 3D E-field patterns (a) Single antenna, (b) 2x1 array

6. CONCLUSION

The 2x1 array with WFN with 3D printing and metal plating technique is fabricated. We have simulated and measured antenna performances for single antenna and 2x1 array. The number of array is proportional to ohmic and reflection losses of array. The gain is increased by approximately1.5dB in comparison with single antenna. However, VSWR of the single antenna is 0.3dB lower than the array antenna. By means of this 3D printing technology and copper plating, it is possible to fabricate the passive components such as waveguide filter, antenna and adaptor 90% lighter weight and 80% cheaper than metal equivalents. It is utilized the T-junction waveguide in order to make the impedance matching. We can design a different number of waveguide feeding network by using this T-junction structure.

References

[1] C. A. Balanis, *Horn Antennas: Antenna Theory: Analysis and Design*. New York: John Wiley & Sons, 2005.

[2] T. S. Bird, *Fundamentals of Aperture Antennas And Arrays: From Theory to Design, Fabrication and Testing*. New York: John Wiley & Sons, 2016.

[3] M. Long, and B. Blake, *Antennas: Fundamentals, Design, Measurement*. London: The Institution of Engineering and Technology, 2009.

[4] P. T. Timbie *et. al.*, "Stereolithographed mm-Wave Corrugated Horn Antennas," in *2011 Proc. 36th Int. Conf. on Infrared, Millimeter, and Terahertz Waves (IRMMW-THz)*, 2011, pp. 1-3.

[5] M. Liang *et al.*, "A 3-D luneburg lens antenna fabricated by polymer jetting rapid prototyping," *IEEE Trans. Antennas Propag.*, vol. 62, pp. 1799-1807, 2009.

[6] W. Whittow, C. Njoku, and J. Vardaxoglou, "Patch Antennas with Heterogeneous Substrates and Reduced Material Consumption Enabled by Additive Manufacturing Techniques," in *2012 IEEE International Symposium on Antennas and Propagation and USNC URSI National Radio Science Meeting*, 2012, pp. 1-4.

[7] B. Sanz-Izquierdo, E. A. Parker, "3-D printing of elements in frequency selective arrays," *IEEE Trans. Antennas Propag.*, vol. 62, pp. 6060-6066, 2014.

[8] I. Gibson, D. Rosen, and B. Stucker, *Additive Manufacturing Technologies Rapid Prototyping to Direct Digital Manufacturing*, Basel: Springer, 2010.

[9] K. T. Selvan, "Accurate design method for optimum gain pyramidal horns," *Electron. Lett.*, vol. 35, pp. 249-250, 1999.

[10] A. I. Dimitriadis *et al.*, "Design and Fabrication of a Lightweight Additive-Manufactured Ka-Band Horn Antenna Array," in *2016 10th European Conference on Antennas and Propagation (EuCAP)*, 2016, pp.1-4.

[11] S. Ördek, and A. Kizilay, "Horn Array Antenna Design for Ku-Band Applications," in *2015 9th International Conference on Electrical and Electronics Engineering (ELECO*), 2015, pp. 351-354.

[12] A. I. Dimitriadis et al., "Polymer-based Additive Manufacturing of High-Performance Waveguide and Antenna Components," in *2017 Proceedings of the IEEE*, 2017, vol. 105, pp. 668-676.

[13] J. C. S. Chieh, B. Dick, and S. Loui, "Development of a Ku-band corrugated conical horn using 3-D print technology," *IEEE Antennas Wirel. Propag. Lett.*, vol. 13, pp. 201-204, 2017.

[14] M. Van der Vorst, and J. Gumpinger, "Applicability of 3D Printing Techniques for Compact Ku-Band Medium/High-Gain Antennas," in *2016 10th European Conference on Antennas and Propagation (EuCAP)*, 2016, pp. 1-4.

[15] K. Güney, "A new design method for optimum gain pyramidal horns," Electromagnetics, vol. 21, pp. 497-505, 2001.

[16] K. Güney, "Improved design method for optimum gain pyramidal horns," *Int. J. RF Microwave Comput. Aided Eng.*, vol. 11, pp. 188-193, 2001.

[17] A. Genc, "Impedance Matching of Dielectric Loaded T-Junction in X-Ku Band," in *2016 Proc. Int. Conf. on Signal Processing and Communication Application (SIU)*, 2016, pp. 1-4.

[18] A. Genc *et al.*, "Farkli güç oranlari için dikdörtgen dalga kilavuzu güç bölücülerinin karakteristiklerinin incelenmesi," *Çukurova Üniversitesi Mühendislik Mimarlık Fakültesi Dergisi*, vol. 33, pp. 261-270, 2018.

[19] A. Genc, T. Goksu, and S. Helhel, "Fabrication of 3D printed rectangular waveguide T-junction with in-phase and equal power division," *Microwave Opt. Technol. Lett.*, vol. 60, 2018.

[20] G. O. Mallory, and J. B. Hajdu, *Electroless Plating: Fundamentals and Applications*, Orlando: American electroplaters and surface finishers society inc, 1990.

[21] A. Genc, T. Goksu, S. Helhel, "Investigation of the performances of waveguide bend components fabricated with 3D printing and copper plating," *Journal of the Faculty of Engineering and Architecture of Gazi University*, vol. 34, pp. 801-810, 2018.

[22] C. Garcia *et. al.*, "Effects of extreme surface roughness on 3D printed horn antenna," *Electron. Lett.*, vol. 49, pp. 734-736, 2013.

[23] A. Castro, B. Babakhani, and S. Sharma, "Design and development of a multimode waveguide corrugated horn antenna using 3D printing technology and its comparison with aluminium based prototype," *IET Microwaves Antennas Propag.*, vol. 11, pp. 1977-1984, 2017.